Supporting Information for

Original article

Understanding the physiological functions of the host xenobiotic-sensing nuclear receptors PXR and CAR on the gut microbiome using genetically modified mice

Mallory Little[a], Moumita Dutta[a], Hao Li[b], Adam Matson[c], Xiaojian Shi[d], Gabby Mascarinas[a], Bruk Molla[a], Kris Weigel[a], Haiwei Gu[d,]*, Sridhar Mani[b,]*, Julia Yue Cui[a,]*

[a]*Department of Environmental and Occupational Health Sciences, University of Washington, Seattle, WA 98105, USA*

[b]*Einstein College of Medicine, Bronx, NY 10461, USA*

[c]*University of Connecticut, Hartford, CT 06106, USA*

[d]*Arizona Metabolomics Laboratory, College of Health Solutions, Arizona State University, Phoenix, AZ 85004, USA*

Receive 2 March 2021; received in revised form 29 May 2021; accepted 9 July 2021

*Corresponding authors. Tel.: +1 206 616 4331.

E-mail addresses: juliacui@uw.edu (Julia Yue Cui), haiweigu@asu.edu (Haiwei Gu), sridhar.mani@einstein.yu.edu (Sridhar Mani).

Section 1 Supporting tables.

Table S1 Optimized UPLC–MS/MS gradient for bile acid chromatography.

Time (min)	Mobile phase A (%) (10 mmol/L ammonium acetate with 20% acetonitrile in water)	Mobile phase B (%) (10 mmol/L ammonium acetate with 80% acetonitrile in water)
0.00	95	5
5.00	95	5
14.00	86	14
14.50	75	25
17.50	75	25
18.00	50	50
22.00	50	50
22.50	20	80
24.50	20	80
25.00	95	5

Table S2 Primer sequences.

qPCR Target	Forward primer (5′–3′)	Reverse primer (5′–3′)
Bile salt hydrolase (*Bsh*)	ATGGGCGGACTAGGATTACC	TGCCACTCTCTGTCTGCATC
L. acidophilus	AGCGAGCTGAACCAACAGAT	TGATCATGCGATCTGCTTTC
L. johnsonii	GAGCGAGCTTGCCTAGATGA	ATCGCCTTGGTAAGCCATTA
Il-6	CCGGAGAGGAGACTTCACAG	TCCACGATTTCCCAGAGAAC
Il-2	GAGTCAGCAACTGTGGTGGA	AGGGCTTGTTGAGATGATGC
Il-12p35	CTCCTGTGGGAGAAGCAGAC	CAGATAGCCCATCACCCTGT

Table S3 Bacteria commonly regulated across *PXR*-null *vs.* WT and *CAR*-null *vs.* WT comparisons.

Adolescent males	Adult males	Adolescent females	Adult females
Anaerostipes sp.	*Anaerostipes* sp.	*Anaerostipes* sp.	*Anaerostipes* sp.
Akkermansia muciniphila	*Dehalobacterium* sp.	*Akkermansia muciniphila*	Mogibacteriaceae family
Mucispirillum shaedleri	*Bacteroides acidifaciens*	*Bacteroides* sp.	*Bacteroides* sp.
Helicobacter sp.	*Helicobacter* sp.	*Anaeroplasma* sp.	*Helicobacter* sp.
Helicobacteraceae family	Helicobacteraceae family	*Enterococcus* sp.	Helicobacteraceae family
Oscillospira sp.	*Sutterella* sp.	*Lactococcus* sp.	*Lactococcus* sp.
Clostridiales order	*Parabacteroides* sp.	*Carnobacterium* sp.	*Parabacteroides* sp.
	S24-7 family (now Muribaculaceae)		

Section 2 Supporting figures

Figure S1

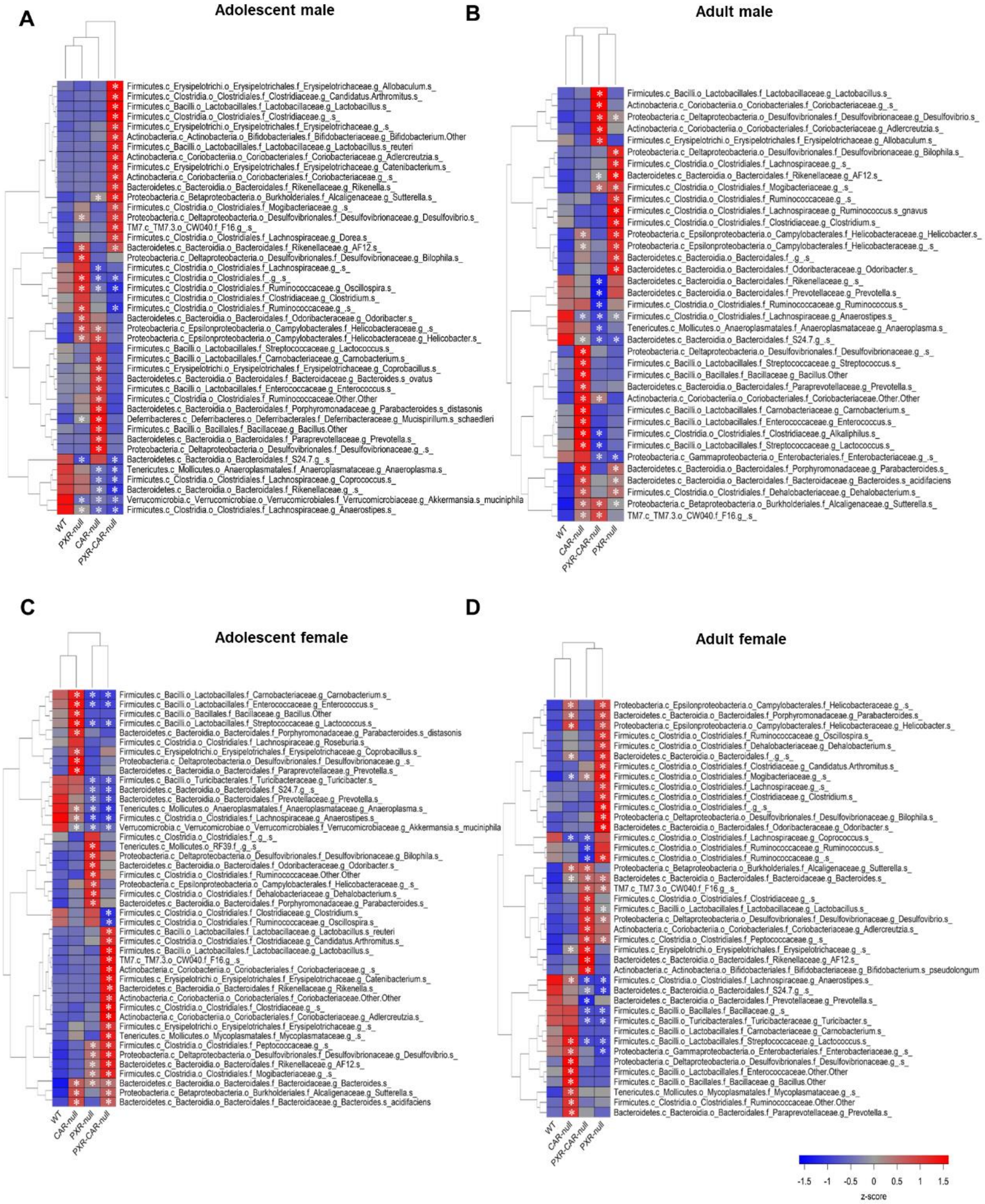

Figure S1 Differentially abundant taxa in C57BL/6 WT, *PXR*-null, *CAR*-null, and *PXR-CAR*-null mice. Two-way hierarchical clustering of the mean differentially abundant taxa in fecal samples from adolescent- and adult-aged male and female C57BL/6 WT, *PXR*-null, *CAR*-null, and *PXR-CAR*-null mice, as generated by the R packages gplots and RColorBrewer.

Asterisks (*) represent statistically significant differences compared to WT mice (one-way ANOVA, Duncan's post hoc, $P < 0.05$).

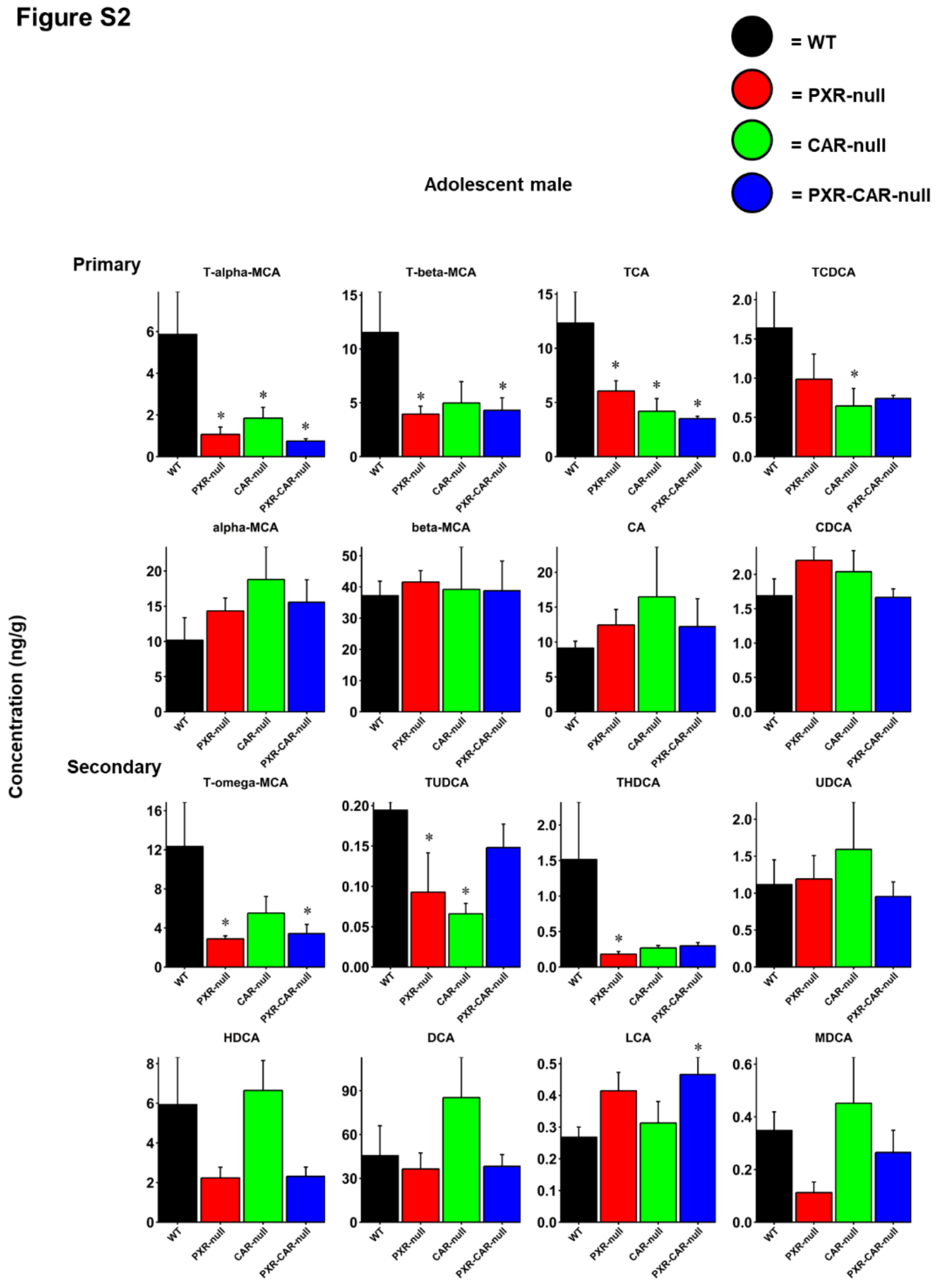

Figure S2 BA concentrations in C57BL/6 WT, *PXR*-null, *CAR*-null, and *PXR-CAR*-null adolescent male mice. Individual bar plots of mean (SE) BA concentrations (ng/g) in adolescent male, mice as generated by the R package ggplot2. BAs were quantified by LC MS/MS as described in Materials and methods. Asterisks (*) represent statistically significant differences compared to WT mice (one-way ANOVA, Duncan's post hoc, $P < 0.05$).

Figure S3

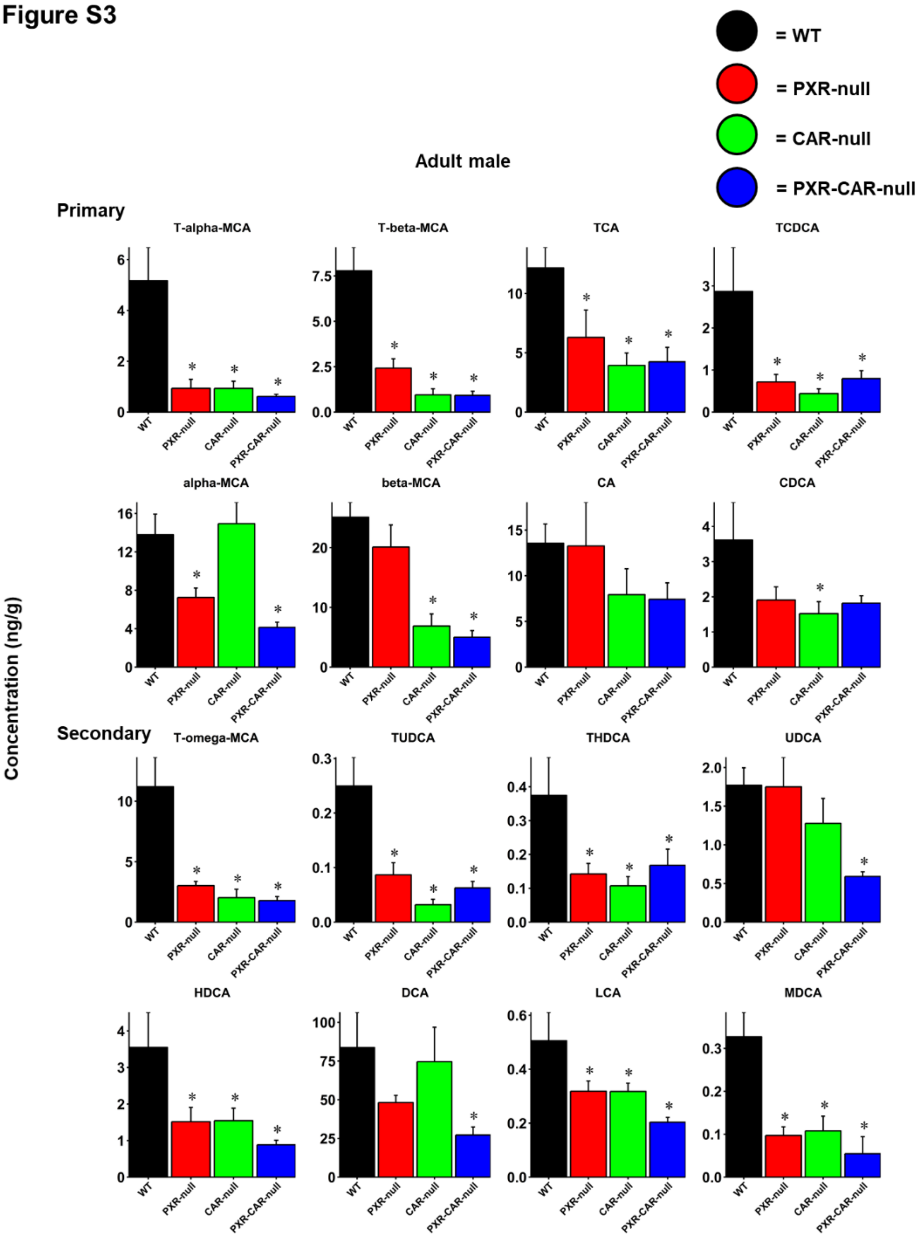

Figure S3 BA concentrations in C57BL/6 WT, *PXR*-null, *CAR*-null, and *PXR-CAR*-null adult male mice. Individual bar plots of mean (SE) BA concentrations (ng/g) in adult male, mice as generated by the R package ggplot2. BAs were quantified by LC–MS/MS as described in Materials and methods. Asterisks (*) represent statistically significant differences compared to WT mice (one-way ANOVA, Duncan's post hoc, $P < 0.05$).

Figure S4

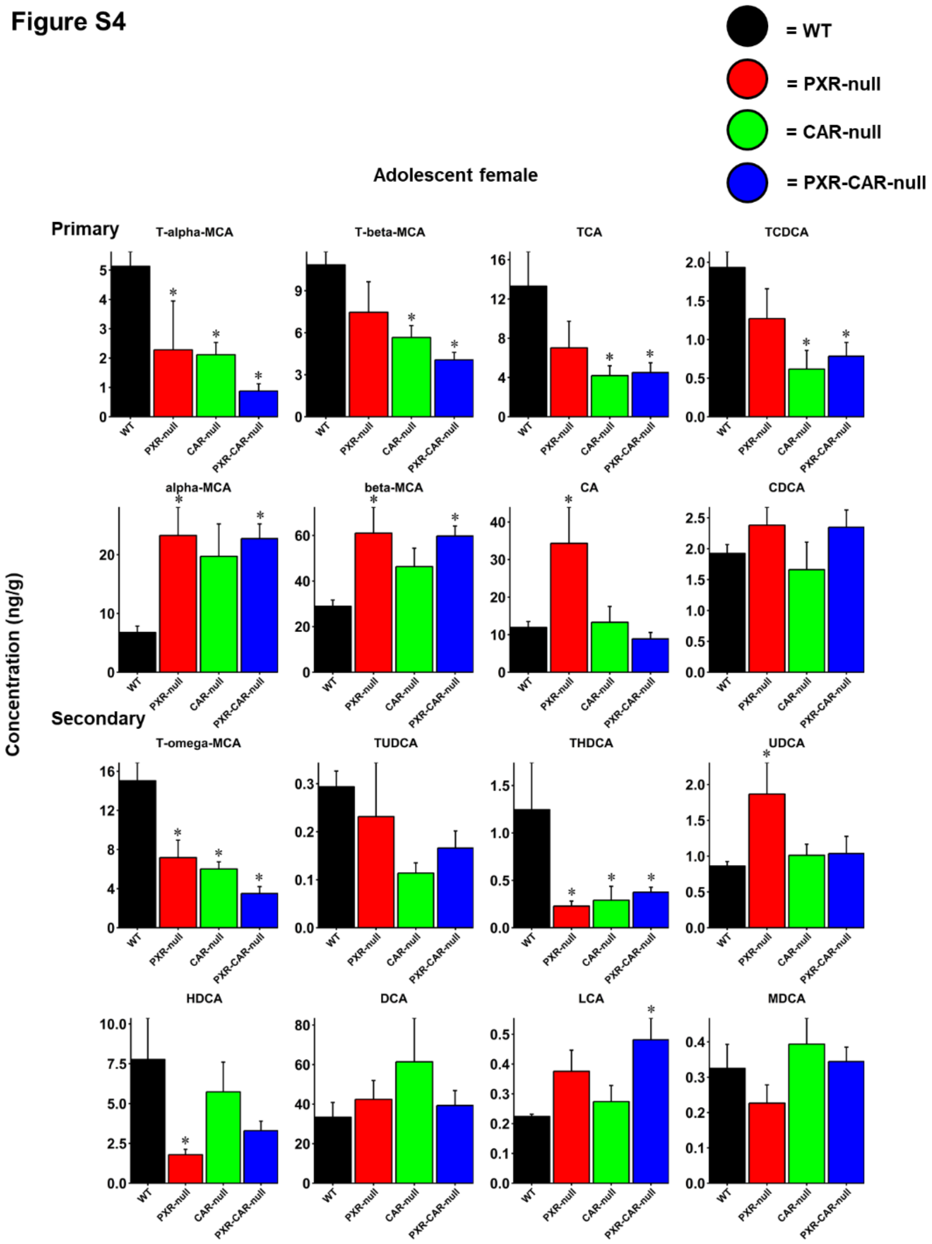

Figure S4 BA concentrations in C57BL/6 WT, *PXR*-null, *CAR*-null, and *PXR-CAR*-null adolescent female mice. Individual bar plots of mean (SE) BA concentrations (ng/g) in adolescent female, mice as generated by the R package ggplot2. BAs were quantified by LC MS/MS as described in Materials and methods. Asterisks (*) represent statistically significant differences compared to WT mice (one-way ANOVA, Duncan's post hoc, $P < 0.05$).

Figure S5

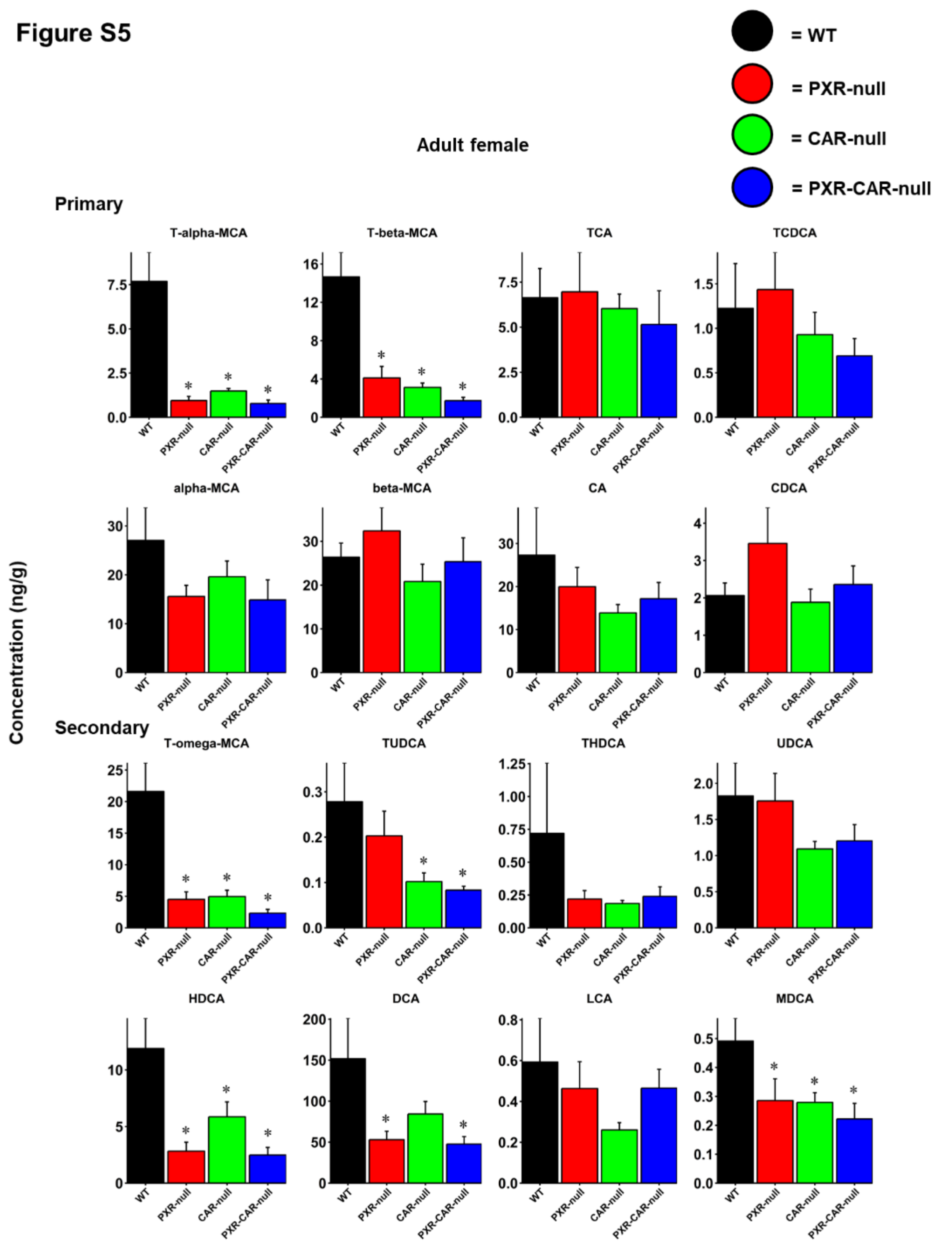

Figure S5 BA concentrations in C57BL/6 WT, *PXR*-null, *CAR*-null, and *PXR-CAR*-null adult female mice. Individual bar plots of mean (SE) BA concentrations (ng/g) in adult female, mice as generated by the R package ggplot2. BAs were quantified by LC–MS/MS as described in Materials and methods. Asterisks (*) represent statistically significant differences compared to WT mice (one-way ANOVA, Duncan's post hoc, $P < 0.05$).

Figure S6

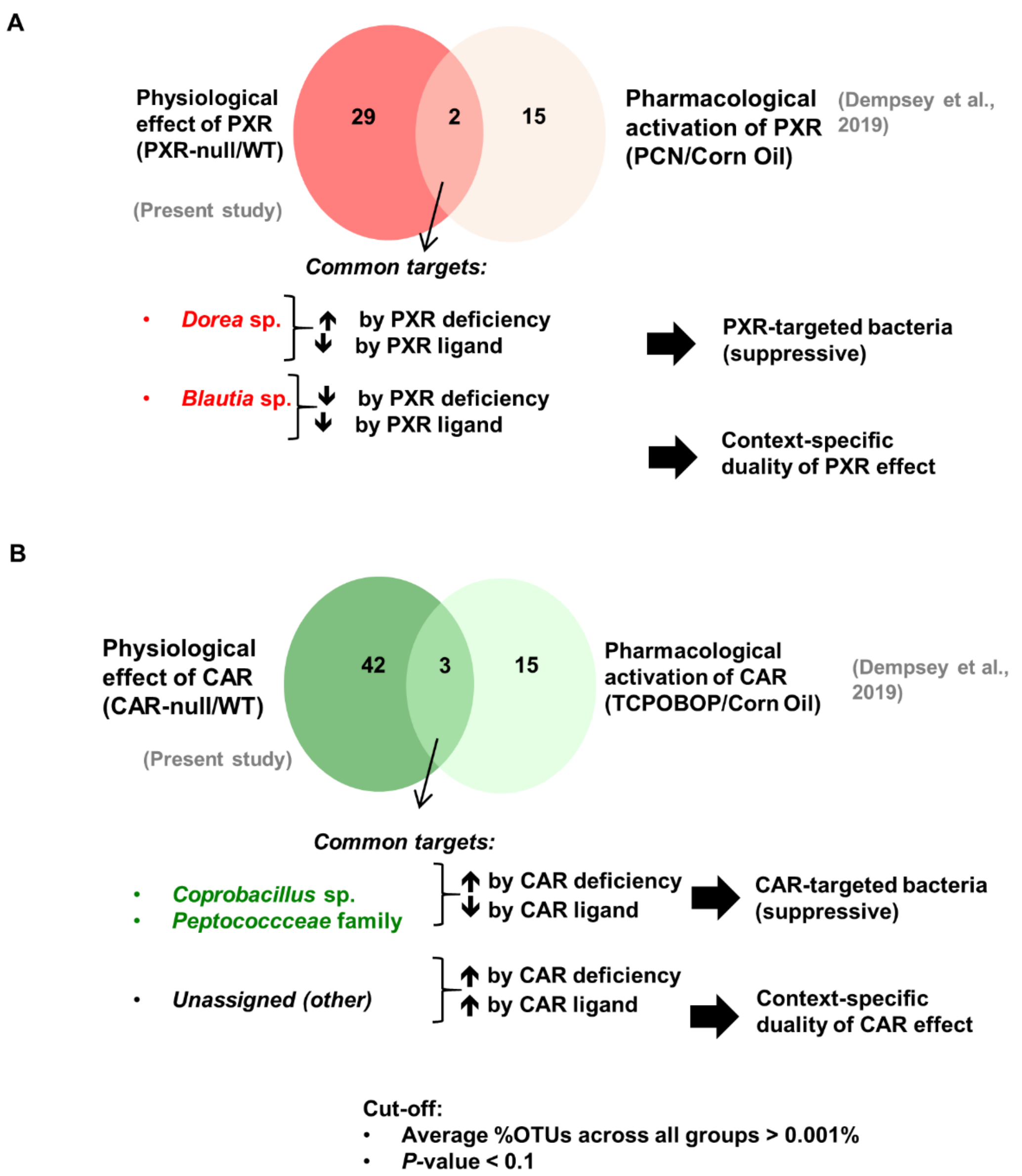

Figure S6 A. Comparison between physiological activation of PXR and pharmacological activation of PXR by its prototypical ligand PCN. Differentially regulated bacteria between *PXR*-null and WT mice of the present study (adult males only) were cross-referenced with a previous 16S rDNA sequencing study where adult C57BL/6 male mice were orally gavaged with the prototypical PXR ligand PCN (75 mg/kg) once daily for 4 consecutive days (PCN *vs*. vehicle [corn oil])[30]. Commonly and uniquely regulated bacteria between the two models are shown in a venn diagram. **B. Comparison between physiological activation of CAR and pharmacological activation of CAR by its prototypical ligand TCPOBOP.** Differentially regulated bacteria between *CAR*-null and WT mice of the present study (adult males only) were cross-referenced with a previous 16S rDNA sequencing study where adult C57BL/6J male mice were orally gavaged with the prototypical CAR ligand TCPOBOP (3 mg/kg) once daily for 4 consecutive days (TCPOBOP vs. vehicle [corn oil])[30]. Commonly and uniquely regulated bacteria between the two models are shown in a venn diagram. The filtering criteria for both A and B are: average % OTUs across all groups > 0.001% in each study, and $P < 0.1$.

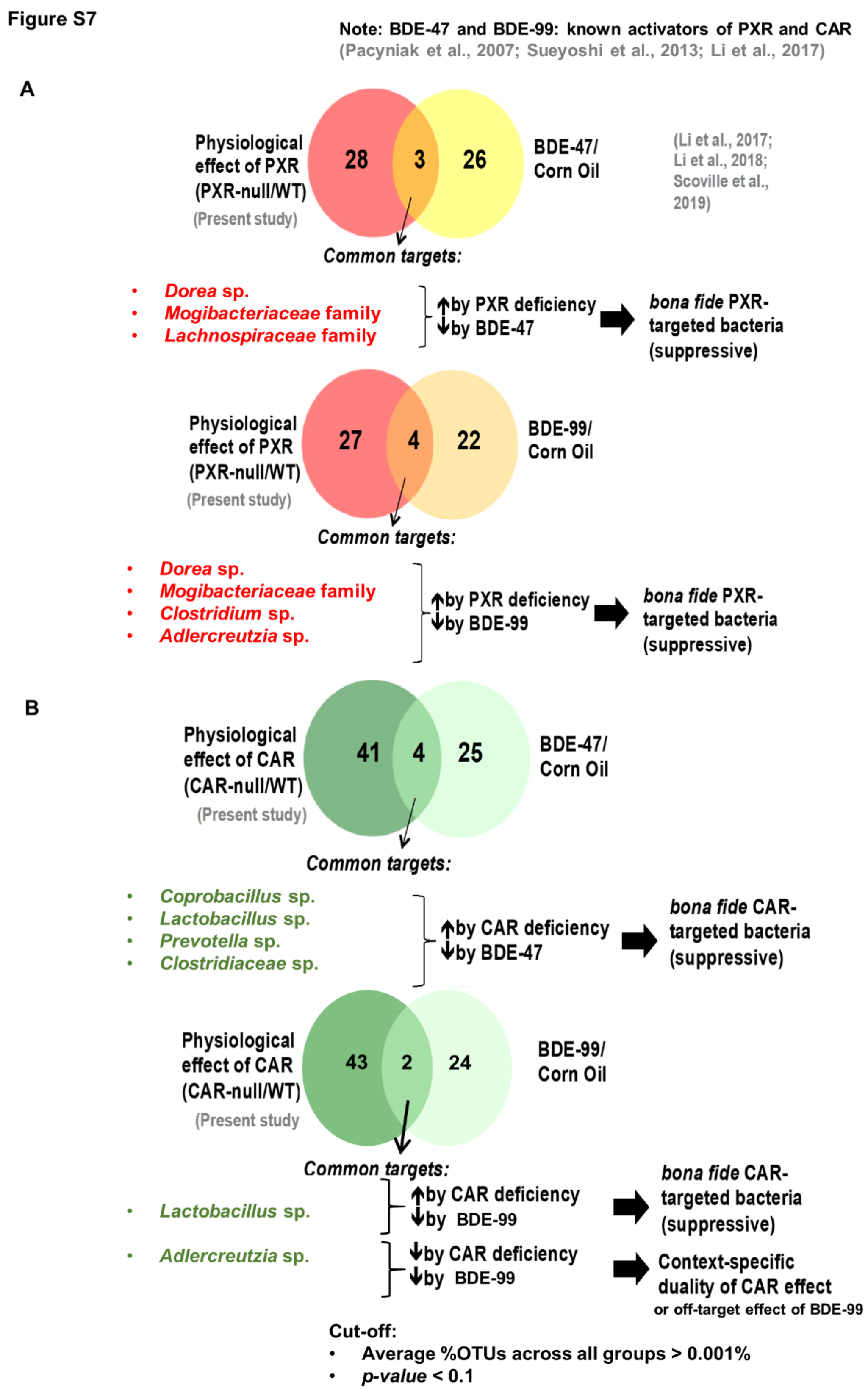

Figure S7 A. Comparison between physiological activation of PXR and toxicological activation of PXR by BDE-47 and BDE-99. Differentially regulated bacteria between *PXR*-null and WT mice of the present study (adult males only) were cross-referenced with a previous

16S rDNA sequencing study where adult C57BL/6 male mice were orally gavaged with BDE-47 or BDE-99 (known activators of PXR, 100 μmol/kg) once daily for 4 consecutive days (PBDEs *vs.* vehicle [corn oil])[9,13,37]. Commonly and uniquely regulated bacteria between the two models are shown in a venn diagram. **B. Comparison between physiological activation of CAR and toxicological activation of CAR by BDE-47 and BDE-99.** Differentially regulated bacteria between *PXR*-null and WT mice of the present study (adult males only) were cross-referenced with a previous 16S rDNA sequencing study where adult C57BL/6 male mice were orally gavaged with BDE-47 or BDE-99 (known activators of CAR, 100 μmol/kg) once daily for 4 consecutive days (PBDEs vs. vehicle [corn oil])[9,13,37]. Commonly and uniquely regulated bacteria between the two models are shown in a venn diagram. The filtering criteria for both A and B are: average % OTUs across all groups > 0.001% in each study, and $P < 0.1$.

Figure S8

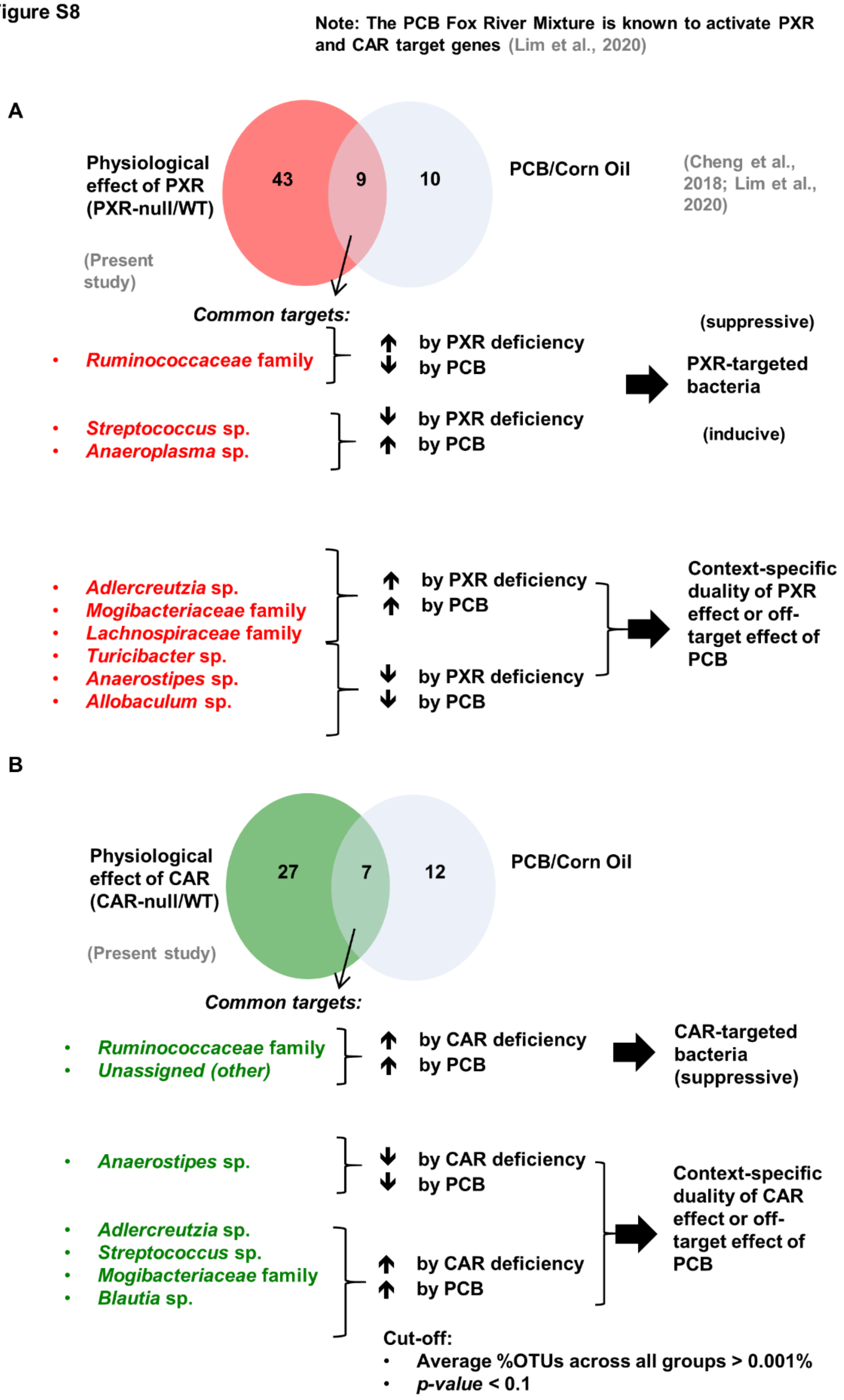

Figure S8 A. Comparison between physiological activation of PXR and toxicological activation of PXR by PCBs. Differentially regulated bacteria between *PXR*-null and WT mice of the present study (adult females only) were cross-referenced with a previous 16S rDNA sequencing study where adult C57BL/6 female mice were orally gavaged with the Fox River PCB mixture (known activators of PXR, 6 mg/kg) once daily for 3 consecutive days (PCBs *vs*. vehicle [corn oil])[31,40]. Commonly and uniquely regulated bacteria between the two models are shown in a venn diagram. **B. Comparison between physiological activation of CAR and toxicological activation of CAR by PCBs.** Differentially regulated bacteria between *CAR*-null and WT mice of the present study (adult females only) were cross-referenced with a previous 16S rDNA sequencing study where adult C57BL/6 female mice were orally gavaged with the Fox River PCB mixture (known activators of PXR, 6 mg/kg) once daily for 3 consecutive days (PCBs vs. vehicle [corn oil])[31,40]. Commonly and uniquely regulated bacteria between the two models are shown in a venn diagram. The filtering criteria for both A and B are: average % OTUs across all groups > 0.001% in each study, and $P < 0.1$.

Figure S9

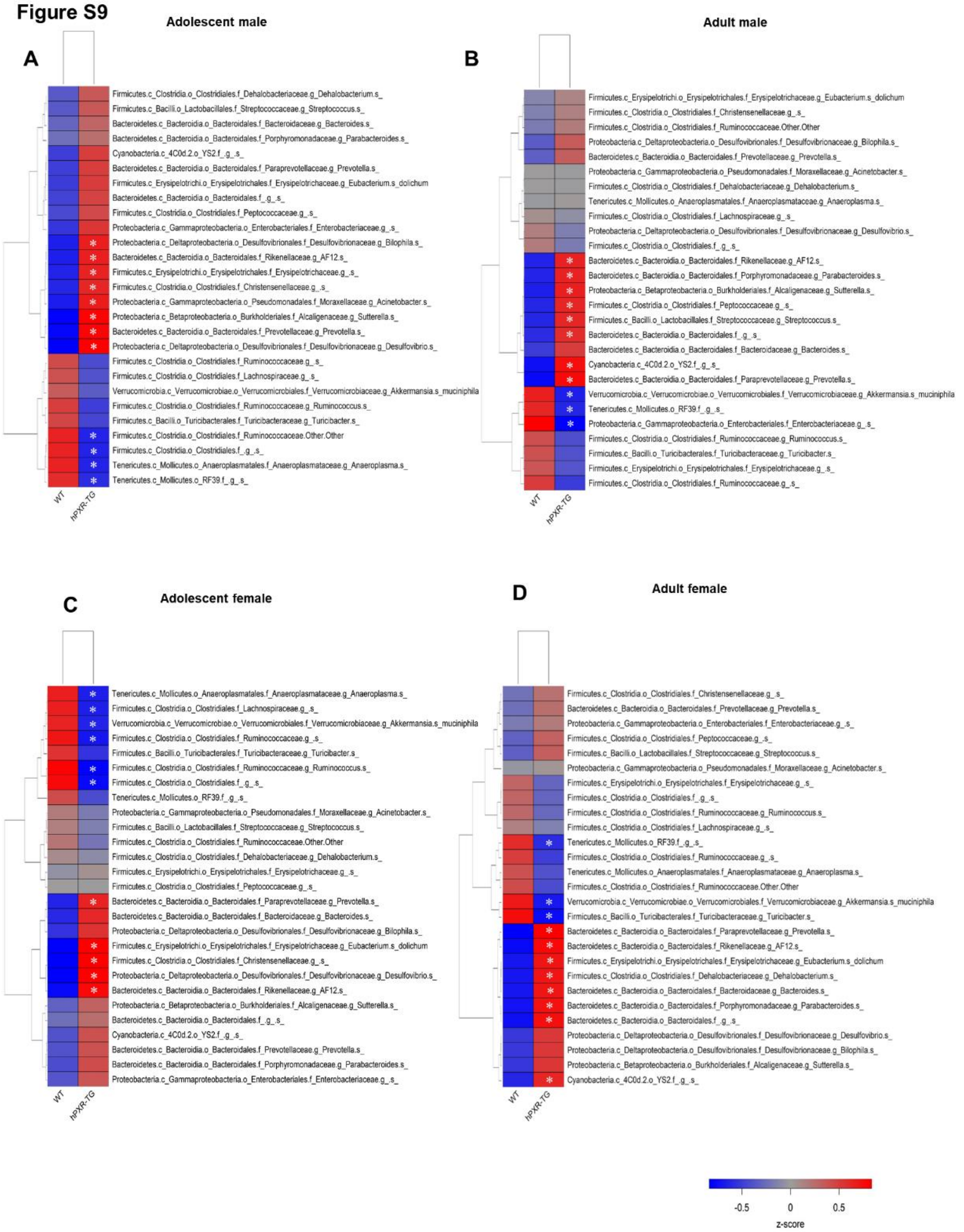

Figure S9 Differentially abundant taxa in WT and h*PXR*-TG FVB/NJ mice. Two-way hierarchical clustering of the mean differentially abundant taxa in fecal samples from adolescent- and adult-aged male and female WT and h*PXR*-TG FVB/NJ mice, as generated by the R packages gplots and RColorBrewer. Asterisks (*) represent statistically significant differences compared to WT mice (*t*-test, $P < 0.05$).

Figure S10

Functional predictions

Adult male

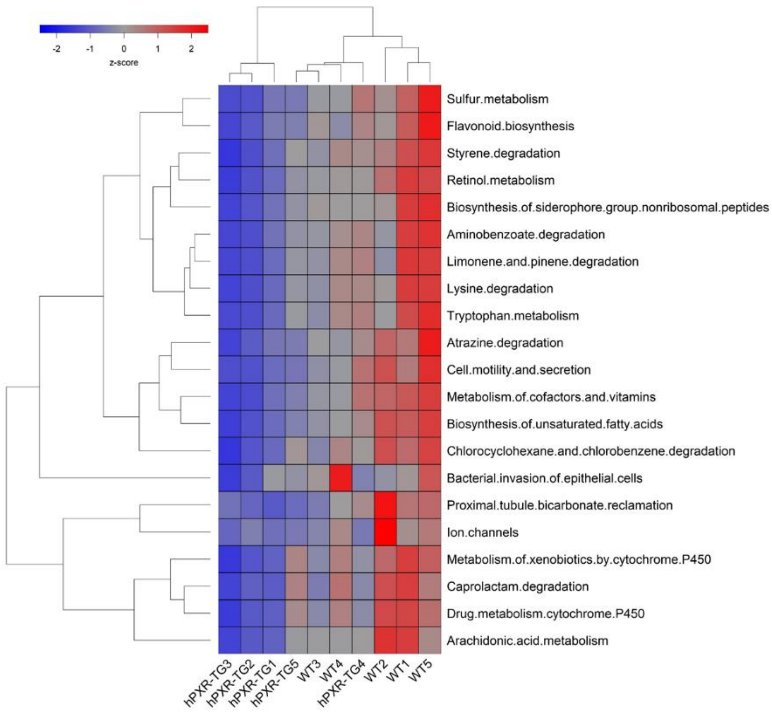

Figure S10. Functional predictions in WT and h*PXR*-TG FVB/NJ mice. Two-way hierarchical clustering dendrograms of differentially regulated KEGG pathways predicted by PICRUSt, as described in Materials and methods, from adolescent- and adult-aged male and female WT and h*PXR*-TG FVB/NJ mice (*t*-test, $P < 0.05$). Generated by the R packages gplots and RColorBrewer.

Figure S11

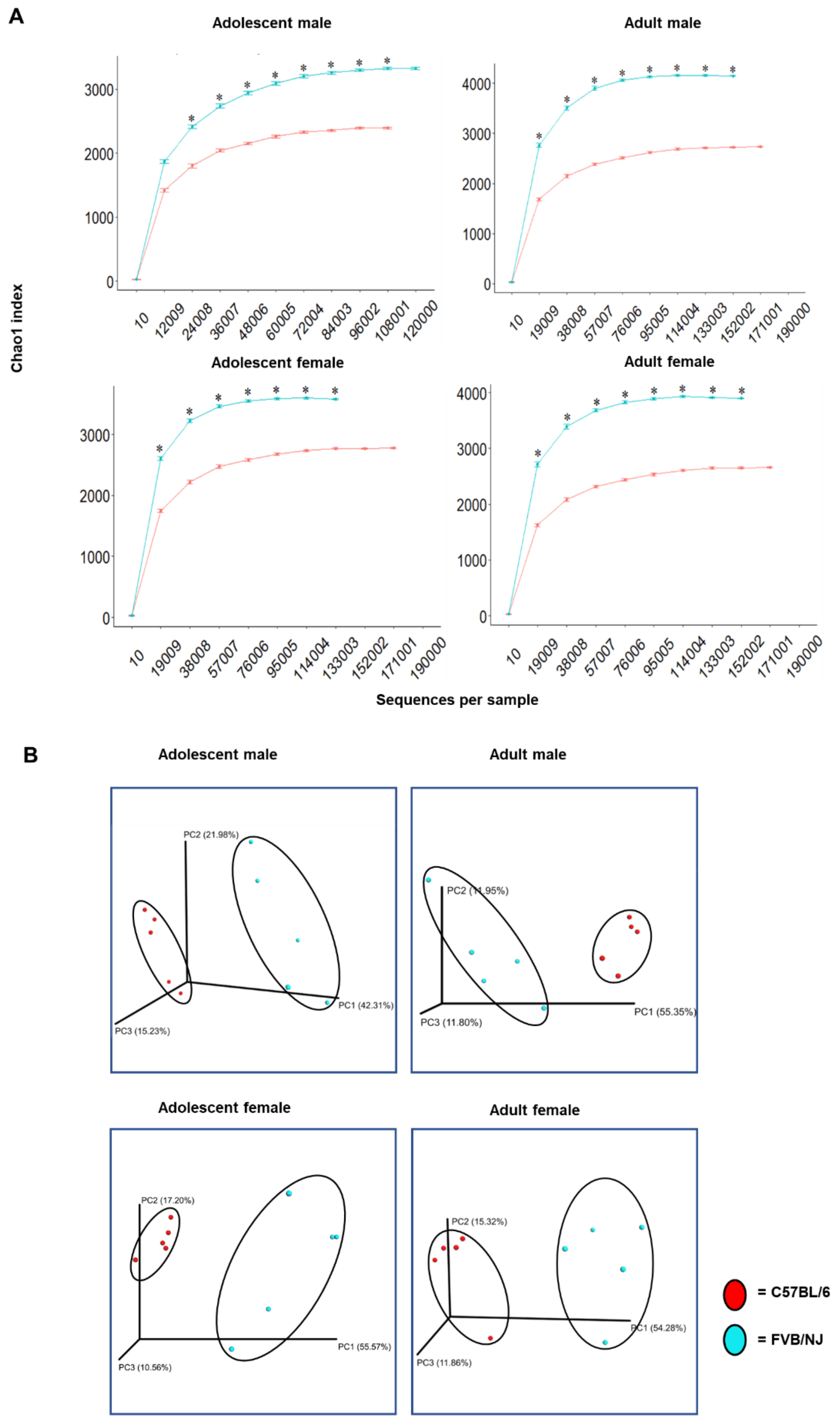

Figure S11 Alpha and beta diversities of C57BL/6 and FVB/NJ mice. A. Mean (SE) alpha diversity of gut microbiota within the low PXR/CAR expressers (C57BL/6) and high PXR/CAR expressers (FVB/NJ mice). Line plots were generated using the R package ggplot.

Asterisks (*) represent statistically significant differences compared to C57BL/6 mice (*t*-test, $P < 0.05$). **B.** Principal coordinate analysis (PCoA) plots showing the beta diversities of adolescent male, adult male, adolescent female, and adult female C57BL/6 and FVB/NJ mice.

Figure S12

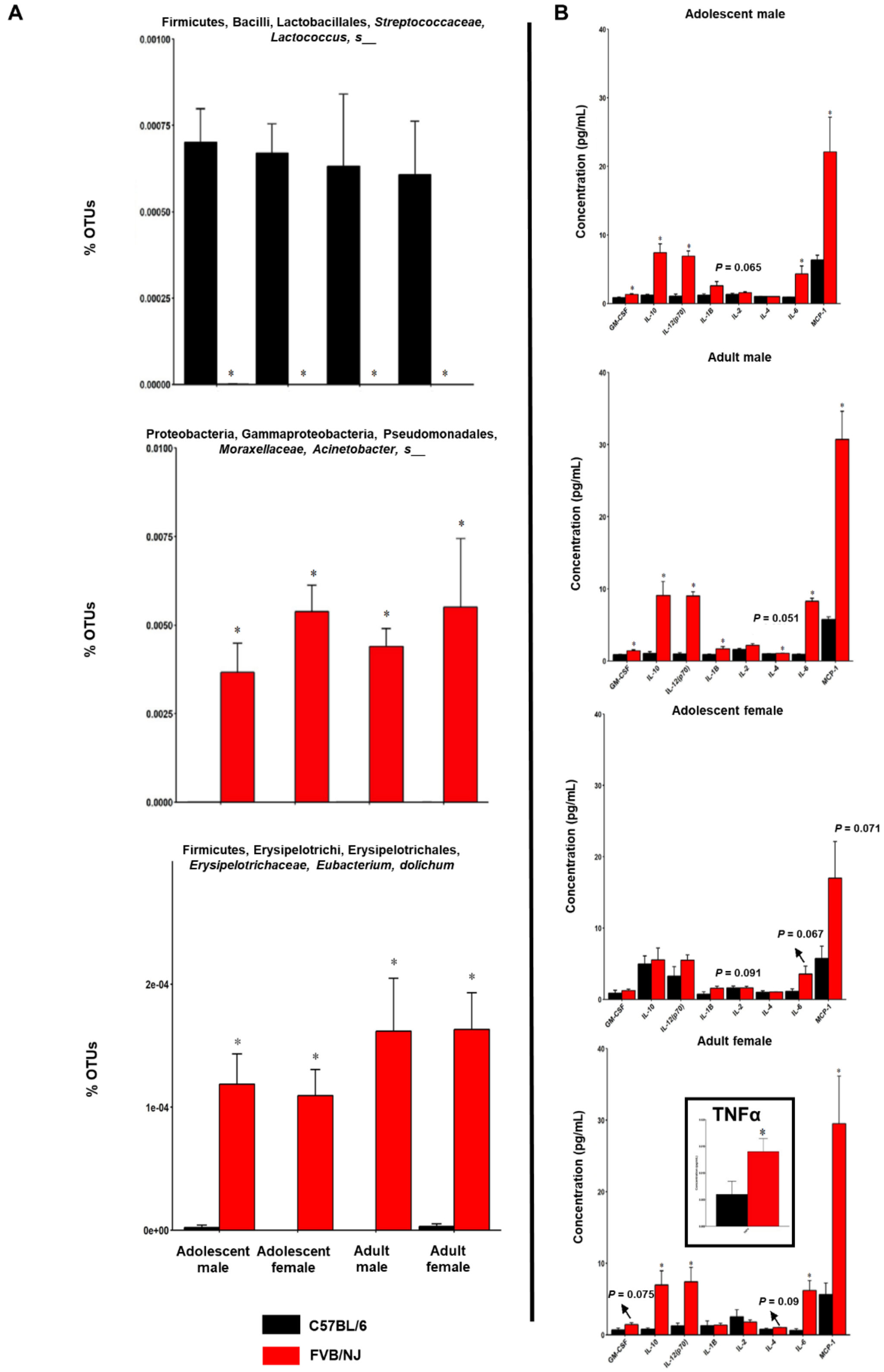

Figure S12 Percentage OTUs of *Lactococcus sp*., *Acinetobacter sp*., and *E. dolichum*, and cytokine concentrations in C57BL/6 and FVB/NJ mice. A. Individual bar plots of mean (SE) percentage OTUs of *Lactococcus sp*., *Acinetobacter sp*., and *E. dolichum*, are generated by the

R package ggplot2. Asterisks (*) represent statistically significant differences compared to C57BL/6 mice (*t*-test, $P < 0.05$). **B.** Bar plots of cytokine concentrations (pg/mL) are generated by the R package ggplot2. Asterisks (*) represent statistically significant differences compared to C57BL/6 mice (*t*-test, $P < 0.05$).

Figure S13

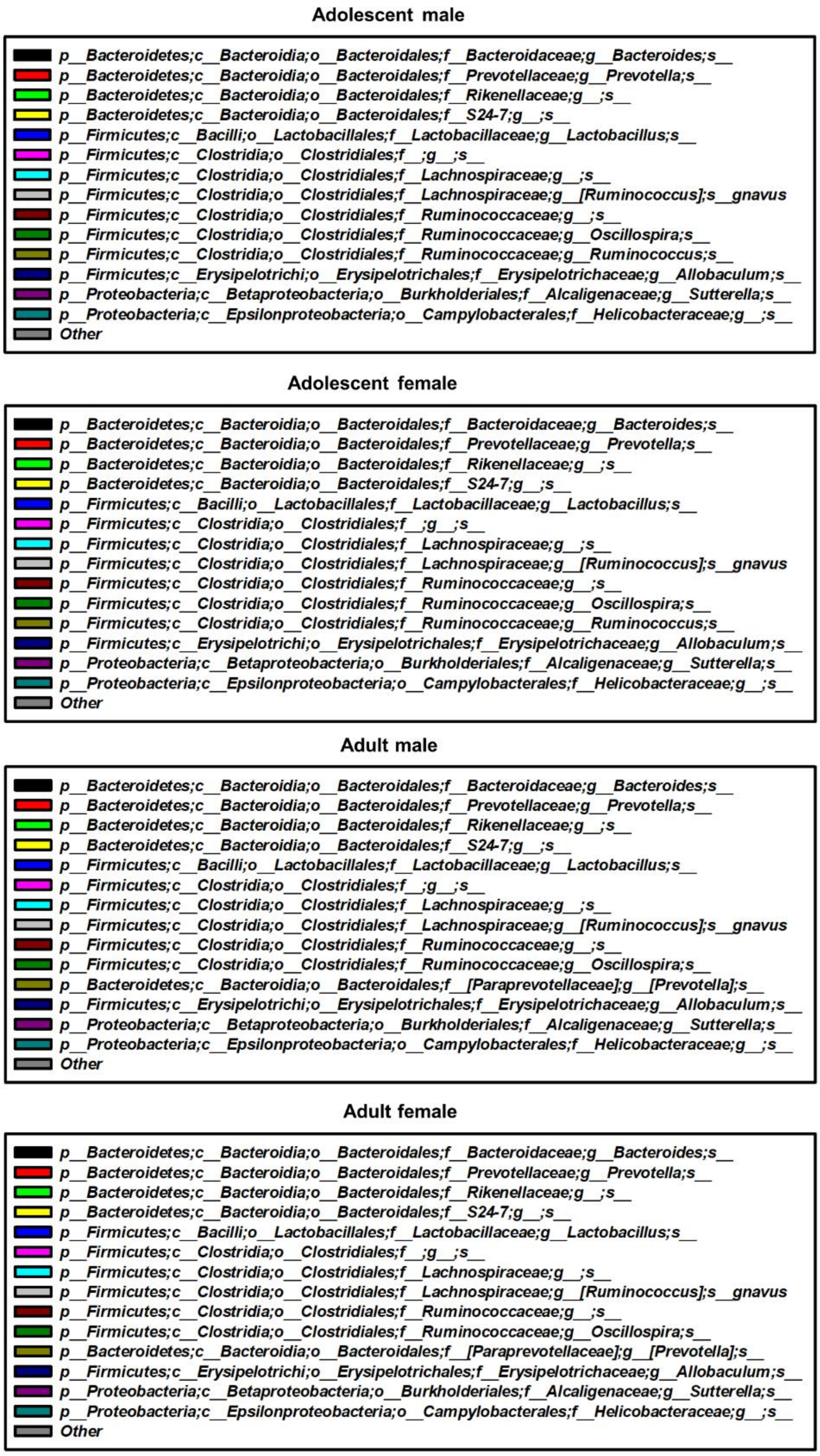

Figure S13 Figure legend for Fig. 3.

Figure S14

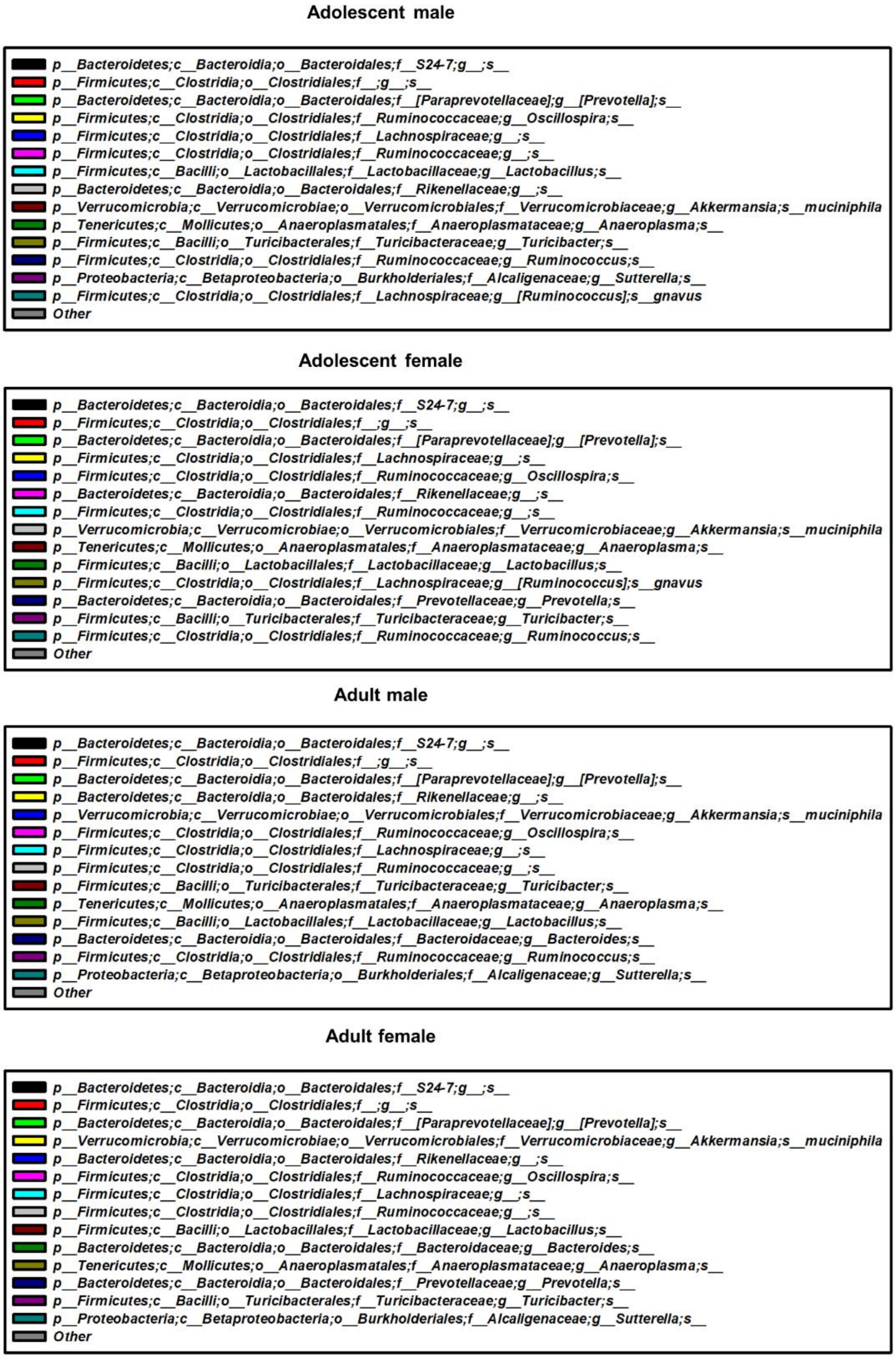

Figure S14 Figure legend for Fig. 8.

Figure S15

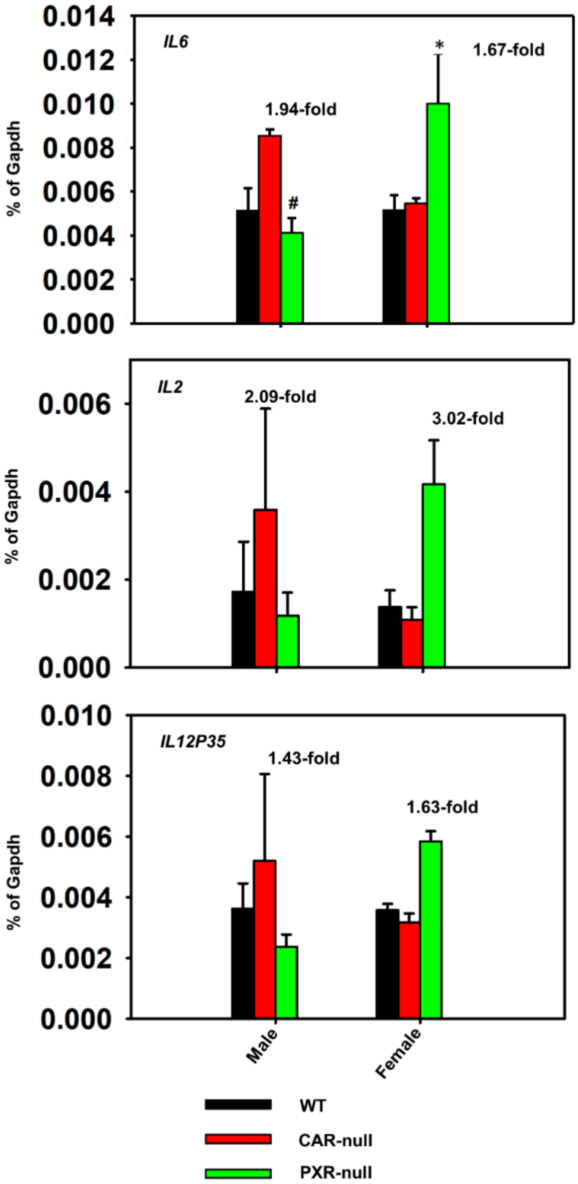

Figure S15 RT-qPCR of liver cytokines in adult WT, *CAR*-null, and *PXR*-null mice. Mean (SE) data are expressed at % of the house-keeping gene *Gapdh*. Asterisks (*) represent statistically significant differences compared to controls, and pound symbols (#) represent statistically significant sex differences (two-way ANOVA, $P < 0.05$).

Figure S16

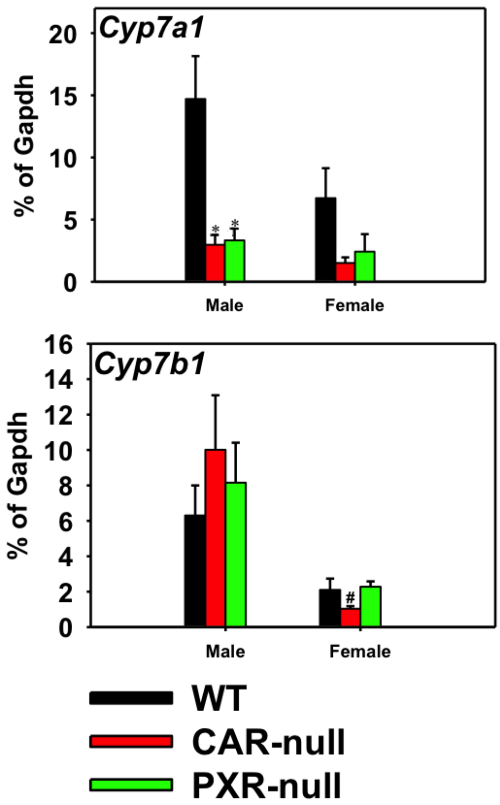

Figure S16 RT-qPCR of BA synthesis enzymes in adult WT, *CAR*-null, and *PXR*-null mice.

Mean (SE) data are expressed at % of the house-keeping gene *Gapdh*. Asterisks (*) represent statistically significant differences compared to controls, and pound symbols (#) represent statistically significant sex differences (two-way ANOVA, $P < 0.05$).